Chaos
An Interdisciplinary Journal of Nonlinear Science

RESEARCH ARTICLE | JANUARY 10 2025

Dynamical properties of the composed Logistic–Gauss map

Special Collection: From Sand to Shrimps: In Honor of Professor Jason A. C. Gallas

Luam Silva de Paiva ; Julia G. S. Rocha ; Joelson D. V. Hermes ; Matheus Hansen ; Ricardo Luiz Viana ; Iberê Luiz Caldas ; Rene O. Medrano-T ; Diogo Ricardo da Costa

Check for updates

Chaos 35, 013129 (2025)
https://doi.org/10.1063/5.0238591

View Online
Export Citation

Articles You May Be Interested In

A recursive method to find the extreme and superstable curves in the parameter space of dissipative one-dimensional mappings

Chaos (February 2025)

A note on chaotic unimodal maps and applications

Chaos (August 2006)

Logistic map trajectory distributions: Renormalization-group, entropy, and criticality at the transition to chaos

Chaos (March 2021)

19 February 2025 18:39:51

AIP Publishing

Chaos

Special Topics Open for Submissions

Learn More

AIP Publishing

Dynamical properties of the composed Logistic–Gauss map

Cite as: Chaos 35, 013129 (2025); doi: 10.1063/5.0238591
Submitted: 12 September 2024 · Accepted: 19 December 2024 ·
Published Online: 10 January 2025

View Online Export Citation CrossMark

Luam Silva de Paiva,[1] Julia G. S. Rocha,[1] Joelson D. V. Hermes,[2,3,a)] Matheus Hansen,[4] Ricardo Luiz Viana,[5] Iberê Luiz Caldas,[3] Rene O. Medrano-T,[1,6] and Diogo Ricardo da Costa[3,5]

AFFILIATIONS

[1]Department of Physics, São Paulo State University—UNESP, Rio Claro, SP 13506-900, Brazil
[2]Federal Institute of Education, Science and Technology of South of Minas Gerais—IFSULDEMINAS, Inconfidentes, MG 37576-000, Brazil
[3]Physics Institute, University of São Paulo—USP, São Paulo, SP 05508-090, Brazil
[4]Center for Mathematics and Applications (NOVA Math), NOVA School of Science and Technology, Universidade NOVA de Lisboa, Quinta da Torre, Caparica 2829-516, Portugal
[5]Department of Physics, Federal University of Paraná—UFPR, Curitiba, PR 82590-300, Brazil
[6]Department of Physics, Federal University of São Paulo - UNIFESP, Diadema, SP 09913-030, Brazil

Note: This paper is part of the Focus Issue, From Sand to Shrimps: In Honor of Professor Jason A. C. Gallas.
[a)]**Author to whom correspondence should be addressed:** joelson.hermes@ifsuldeminas.edu.br

ABSTRACT

This study focuses on the analysis of a unique composition between two well-established models, known as the Logistic–Gauss map. The investigation cohesively transitions to an exploration of parameter space, essential for unraveling the complexity of dissipative mappings and understanding the intricate relationships between periodic structures and chaotic regions. By manipulating control parameters, our approach reveals intriguing patterns, with findings enriched by extreme orbits, trajectories that connect local maximum and minimum values of one-dimensional maps. This theory enhances our perception of structural organization and offers valuable perceptions of the system behaviors, contributing to an expanded understanding of chaos and periodicity in dynamic systems. The analysis reveals Complex Sets of Periodicity (CSP) in the parameter space, characterized by superstable curves that traverse their main bodies. The exploration of different combinations of parameters shows cascades of CSP structures with added periods and are organized based on extreme curves. This investigation offers valuable discoveries of the dynamics of dissipative mappings, opening avenues for future explorations in chaotic systems.

Published under an exclusive license by AIP Publishing. https://doi.org/10.1063/5.0238591

19 February 2025 18:39:51

In this paper, we explore a dynamical system model known as the Logistic–Gauss map. This model is a composition of two well-known models that allow us to investigate complex behaviors in dynamical systems. The focus of this research is to reveal how small changes in the control parameters can transform the dynamics of the system, organizing unique patterns and structures that we call Complex Sets of Periodicity (CSP). These CSPs are areas where periodic behavior intersects with chaotic regions, forming truly fascinating patterns. Using bifurcation diagrams and the concept of extreme orbits, we show how the interactions between extreme and superstable curves help to better understand how domains of periodicity are organized and evolves when a control parameter is perturbed. Our findings highlight the importance of these patterns for understanding the transition between regular and chaotic behaviors and suggest that these techniques may be useful for investigating similar phenomena in other dynamical models.

I. INTRODUCTION

When considering the complexity of dynamic systems and the relevance of studying chaotic behaviors, the analysis of mappings stands out as a fundamental tool, attracting the attention of researchers across various disciplines such as physics, mathematics, and chemistry.[1–3] In this context, notable models like the Logistic map, proposed by Robert May in 1976 to model insect populations,[4] and its generalized version, the Logistic-like map,[5] along with the

Published under an exclusive license by AIP Publishing

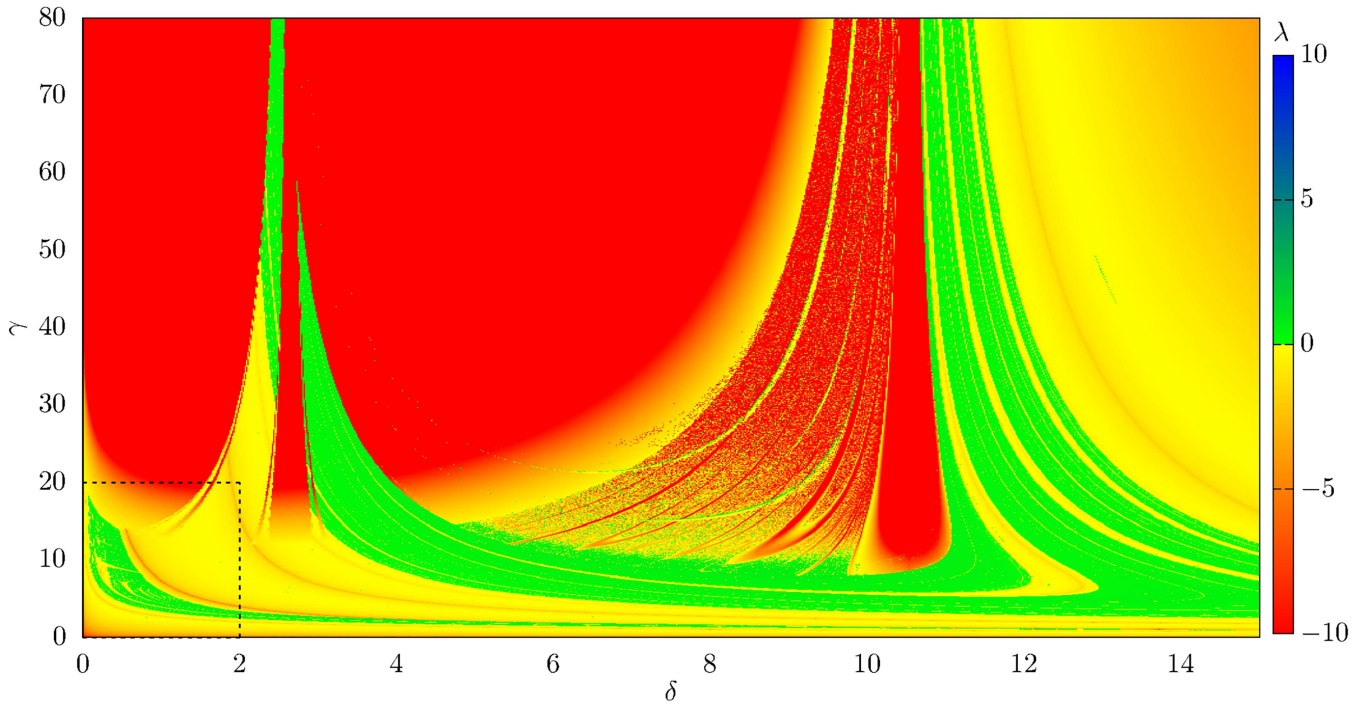


FIG. 1. Parameter space γ vs δ for $\beta = 0.1$. The color palette represents the Lyapunov exponent λ, where the periodic orbits ($\lambda < 0$) are colored as the red/yellow regions, while the chaotic orbits ($\lambda > 0$) receive the green/blue colors.

Gauss map, have been widely explored to understand population growth and other complex phenomena in dynamic systems.[6,7]

Within the scope of this study, our focus is directed toward the analysis of a peculiar map resulting from the composition of these two mappings, known as the Logistic–Gauss map.[8] This choice not only enhances the understanding of the complex phenomena inherent in dynamic systems but also provides room to explore unique properties emerging from the interaction between the Logistic-like map and the Gauss map. The natural transition of this investigation leads us to the exploration of the parameter space, an essential step in unraveling the underlying complexity of these dissipative mappings and understanding the intricate relationships between periodic structures and chaotic regions. By manipulating control parameters, our approach aims to unveil intriguing patterns characterizing the interconnection of these structures, with their comprehension enriched by the application of the theory of extreme orbits, trajectories that connect local maximum and minimum values of one-dimensional maps. This formalism not only refines our perception of the global organization of periodicity domains,[9] the emergence of the period-adding phenomenon,[8] and the understanding of the complexity of the fat fractal between regular and irregular behavior along cascades of periodicity[10] but also yields valuable understandings of the various system behaviors, emerging as a new powerful tool to expand our understanding of chaos in the parameter space of dynamical systems.

In analyzing the parameter space for the model in question, we identified periodic structures embedded in chaotic regions. In this work, we term such periodic structures as Complex Sets of Periodicity (CSP), a term often associated with suggestive descriptions such as shrimps, fishhooks, swallows, and compound windows, among other nomenclatures used in previous studies.[11–14] But, it also includes different domains, namely, spring and saddle-area,[15,16] tricorns,[17,18] and rings.[19] A notable characteristic of some CSP structures is the presence of superstable curves traversing its main body. In practical terms, a CSP structure is defined as continuous regions of periodicity present in the parameter space, which are embedded in chaotic regions. This article demonstrates that the intersection of two extreme curves always occurs in regions where at least one superstable curve coexists. Thus, these intersections of extreme curves provide perceptions of the periodic structures present in the parameter space of the system. Furthermore, by exploring different combinations of control parameters, we observed the emergence of cascades of CSP structures, adding new periods, and the formation of diverse regions that rapidly diverge. We analyze bifurcation diagrams and return maps, essential tools for understanding the mapping dynamics. Bifurcation diagrams highlight the periodicity windows associated with CSP structures and the routes to chaos, while return maps allow us to identify the extreme and superstable orbits related to their respective curves. Additionally, return maps highlight the properties discussed throughout the text, reinforcing

19 February 2025 18:39:51

Published under an exclusive license by AIP Publishing

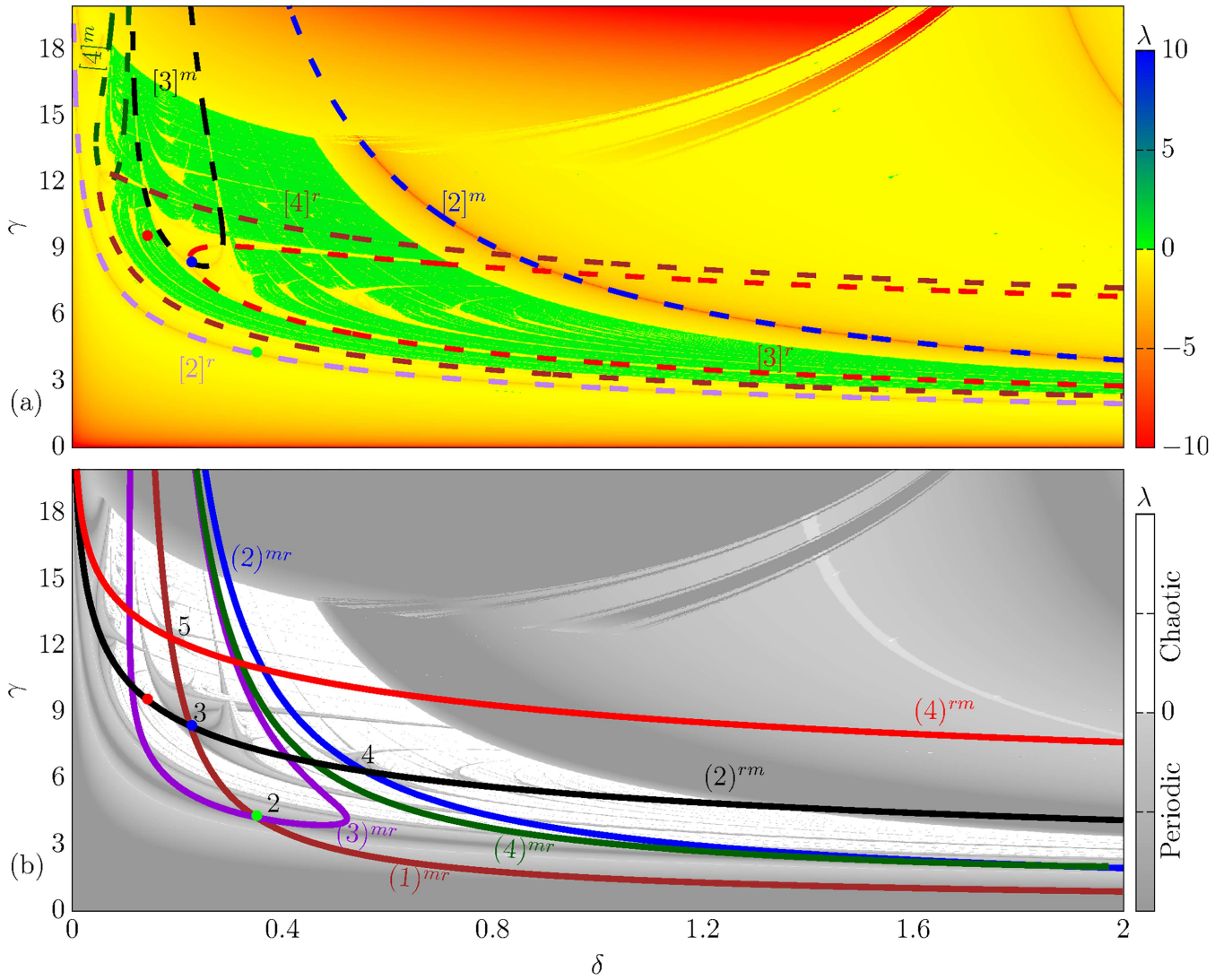


FIG. 2. Parameter space γ vs δ for fixed value of $\beta = 0.1$, where the color scheme represents the value of the Lyapunov exponent. The dashed lines in (a) are superstable curves while the lines in (b) are the extreme curves. The numbers 2, 3, 4, and 5 in (b) correspond to the periodicity of the CSP structures.

the proposed analysis. Thus, these tools provide a deeper understanding of the complex patterns and emergent behaviors in the system.

This paper is organized as follows: in Sec. II, we present the map and show some numerical results. Section III presents a detailed explanation of the results found. Finally, in Sec. IV, we trace our closing remarks.

II. ABOUT THE MAP

The mapping to be studied in this work is based on the coupling of two mappings, referred to as Logistic-like and Gauss.[5,6] The newly created mapping reveals a broad spectrum of information, as discussed in Ref. 8. Among these, it is noteworthy to highlight the CSP structures (Complex Sets of Periodicity) and cyclic curves. The Logistic-like mapping is described as follows:

$$L(x_n) = x_n R\left(1 - x_n^{\gamma}\right), \tag{1}$$

where R and $\gamma > 0$ are control parameters. The Gaussian mapping is written as

$$G(x_n) = \mathrm{e}^{-\alpha x_n^2} + \beta, \tag{2}$$

where α and β are control parameters. The Logistic–Gauss map $F(x_n)$ is the composition $G(L(x_n))$, thus,

$$F(x_n) = \mathrm{e}^{-\delta\left[x_n\left(1-x_n^{\gamma}\right)\right]^2} + \beta, \tag{3}$$

19 February 2025 18:39:51

Published under an exclusive license by AIP Publishing

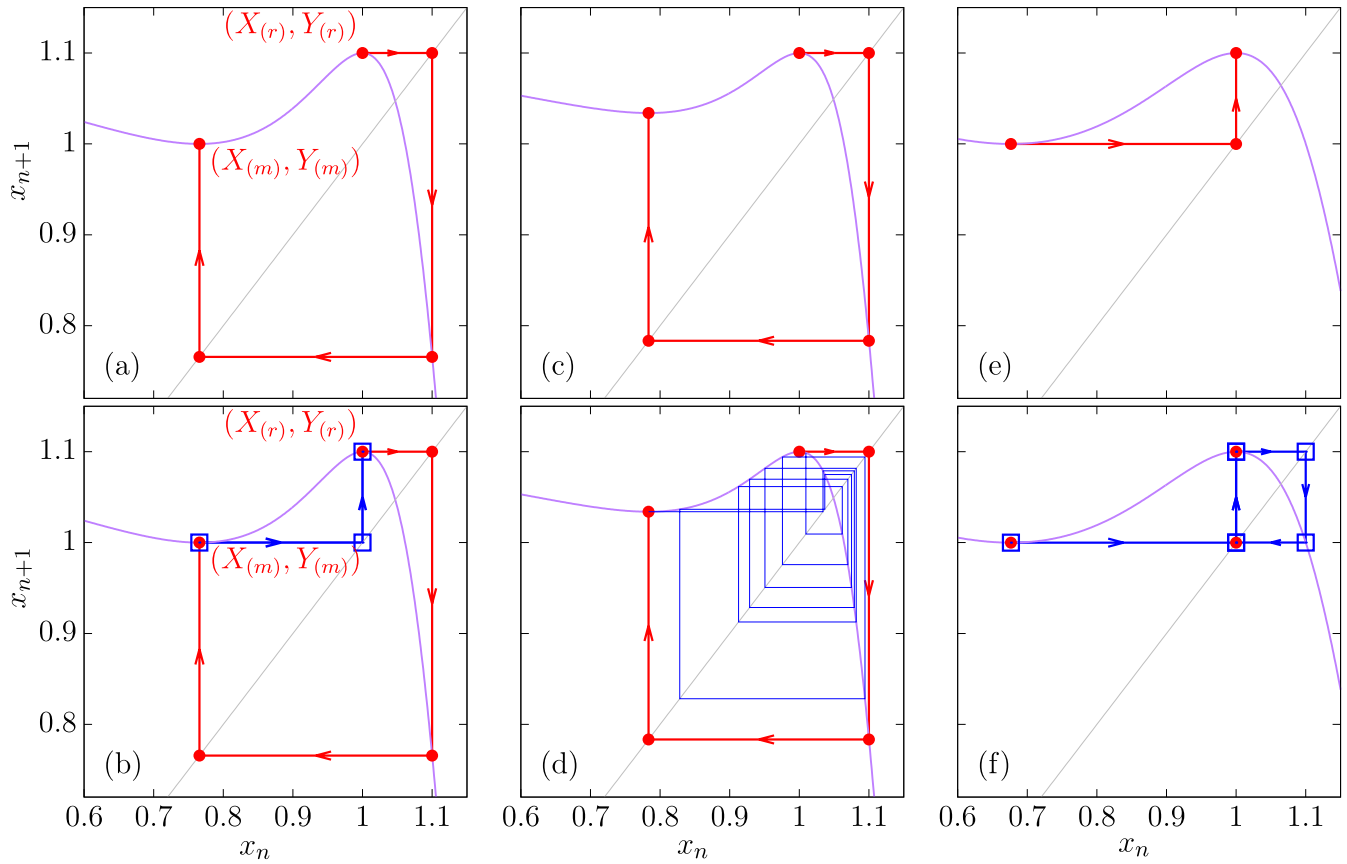


FIG. 3. In (a), we show a particular orbit of the extreme curve $(2)^{rm}$, which connects the maximum $Y_{(r)}$ to the minimum $Y_{(m)}$ after two iterations, while in (b), we present the extreme orbit associated to $(1)^{mr}$ in blue. Something important to note is that the end of each orbit is the beginning of the other giving to a period 3 superstable orbit. Item (c) also shows an extreme orbit associated to $(2)^{rm}$ in red, and in (d), it is possible to notice what happens when we iterate the mapping several times. In this case, the orbit reaches a chaotic attractor. Panel (e) shows an extreme orbit associated to $(1)^{mr}$ in red, while item (f) shows the extreme orbit associated to $(3)^{mr}$ in blue. This orbit leaves the minimum of $Y_{(m)}$ and after three iterates reaches the maximum at $Y_{(r)}$. We used the following combination of control parameters: (a) and (b) $\delta = 0.2253$ and $\gamma = 8.3763$; (c) and (d) $\delta = 0.1353$ and $\gamma = 9.7165$; and (e) and (f) $\delta = 0.3520$ and $\gamma = 4.2353$. For all situations, we have $\beta = 0.1$.

where $\delta = \alpha R^2$ is our new control parameter. So, we have three control parameters that need to be considered: δ, γ, and β. The parameter δ must satisfy $\delta > 0$, as it controls the "width" of the exponential term in the map $F(x_n)$, ensuring a meaningful decay in the system's dynamics. Additionally, γ must be positive, $\gamma > 0$, to guarantee that the term x_n^γ is well-defined and continuous for $x_n \in [0, 1]$. Finally, the parameter β can take any real value, $\beta \in \mathbb{R}$, as it controls the vertical shift of the function, affecting the location of fixed points and the overall dynamics of the system.

To better explore the parameter space ahead, we need to find the local maximum and minimum points of the mapping F. Such points can be found by calculating the solution of $F'(x_n) = 0$, thus, we have

$$F'(x) = -2\delta x\,(1 - x^\gamma)\,[1 - (\gamma + 1)\,x^\gamma]\,\mathrm{e}^{-\delta\left[x(1-x^\gamma)\right]^2} = 0. \quad (4)$$

After solving the previous equation, we find the following solutions:

$$X_{(l)} = 0, \quad X_{(m)} = (1 + \gamma)^{-1/\gamma}, \quad \text{and} \quad X_{(r)} = 1, \quad (5)$$

where $X_{(l)}, X_{(m)}$, and $X_{(r)}$ are critical points of the extremes l, m, r, valid for $\delta \neq 0$ and $\gamma \neq 0$. If γ is a rational number with even numerator, two more critical points come out, $X_{(m^-)} = -X_{(m)}$ and $X_{(r^-)} = -X_{(r)}$. In this context, we call *k-extreme orbits* the trajectories that connect solutions of Eq. (4) after k iterations; therefore, the condition for this orbit is $X_i = F^k(X_j)$. Furthermore, if an extreme point belongs to a periodic orbit, then it belongs to a *superstable orbit*, that is, $X_i = F^k(X_i)$. In bi-dimensional parameter space, a general extreme orbit describes curves called *extreme curves*, which correspond to the set of parameters for which a k-extreme orbit exists. Analogously, a *superstable curve* is a curve in parameter space associated with a general superstable orbit. In this work, we will

19 February 2025 18:39:51

Published under an exclusive license by AIP Publishing

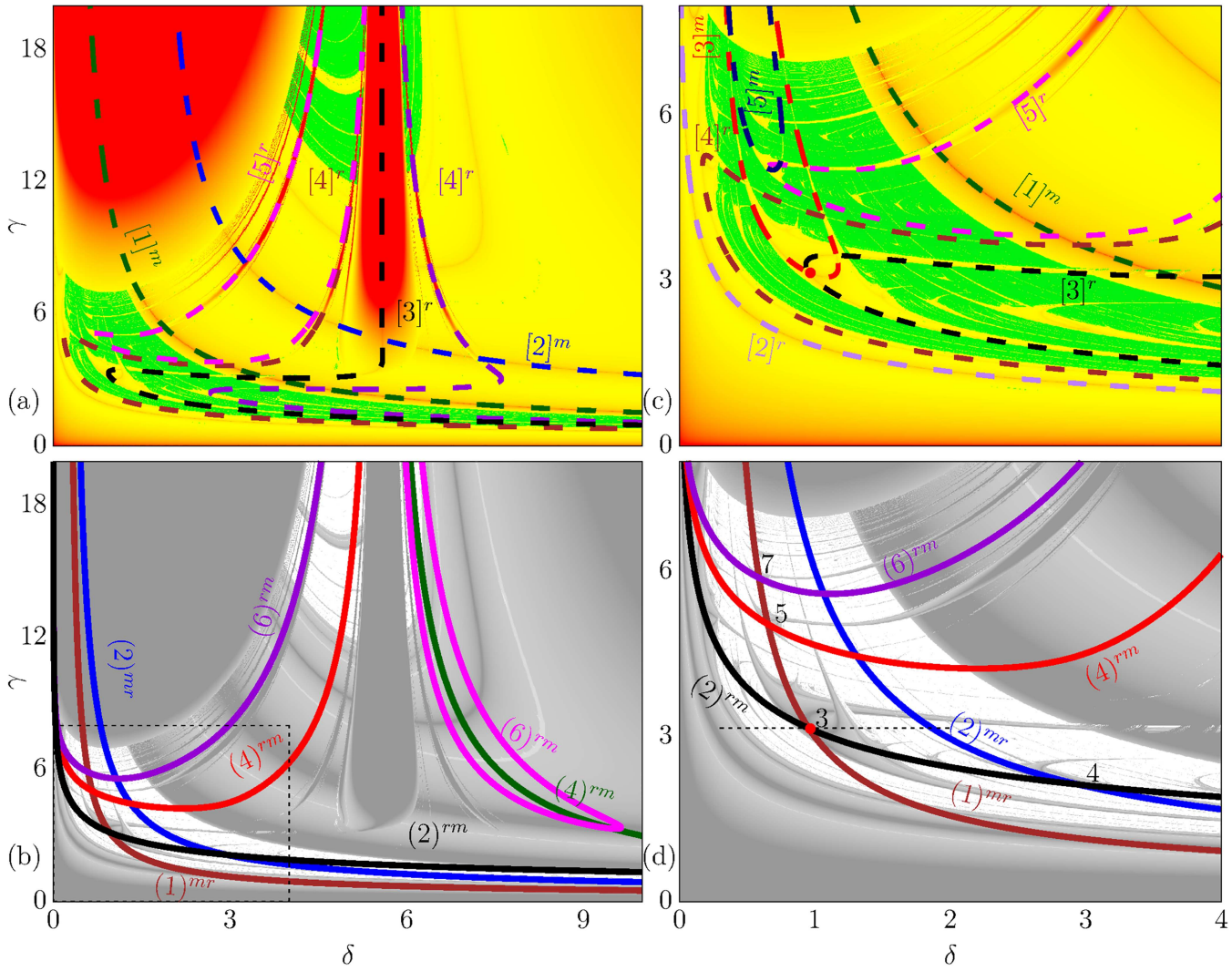


FIG. 4. Parameter space γ vs δ for $\beta = 0.2$. In (a) and (c), we show the superstable curves as the dashed colored lines, where the colors in the parameter space represent the Lyapunov exponent λ. In (b) and (d), we show the extreme curves as the colored lines. In (d), we highlight some numbers that correspond to the periodicity of the CSP structures.

denote a superstable curve by $[u]^i$, which represents that the orbits associated with this curve connect the extreme i to itself after u iterations. On the other hand, an extreme curve will be represented by $(u)^{ij}$, which is associated to the extreme orbit that connects extreme points from i to j after u iterations.

In Secs. III and IV, we explore the properties of the extreme orbits that connect the critical points $X_{(l)}, X_{(m)}$, and $X_{(r)}$.

III. NUMERICAL RESULTS

In Fig. 1, we present the Lyapunov diagram in the parameter space for the mapping F. We considered a grid of 1000×1000 different values for $\delta \in [0, 15]$ and $\gamma \in [0, 80]$, with a fixed $\beta = 0.1$. This broad interval was chosen to provide a general overview, but in future analyses, it will be refined to focus on regions that exhibit structures of interest. For each combination of (δ, γ), the mapping was iterated up to 10^3 times. Subsequently, the Lyapunov exponent was calculated for the next 10^3 iterations. It is noteworthy that the Lyapunov exponent for this mapping is described as follows:

$$\lambda = \frac{1}{M} \sum_{j=1}^{M} \ln \left| F'(x) \right|, \tag{6}$$

where M is the final number of iterations, which is given by $M = 10^3$. This exponent provides important information about the orbit dynamics. For instance, in Fig. 1, a color palette ranging from

19 February 2025 18:39:51

Published under an exclusive license by AIP Publishing

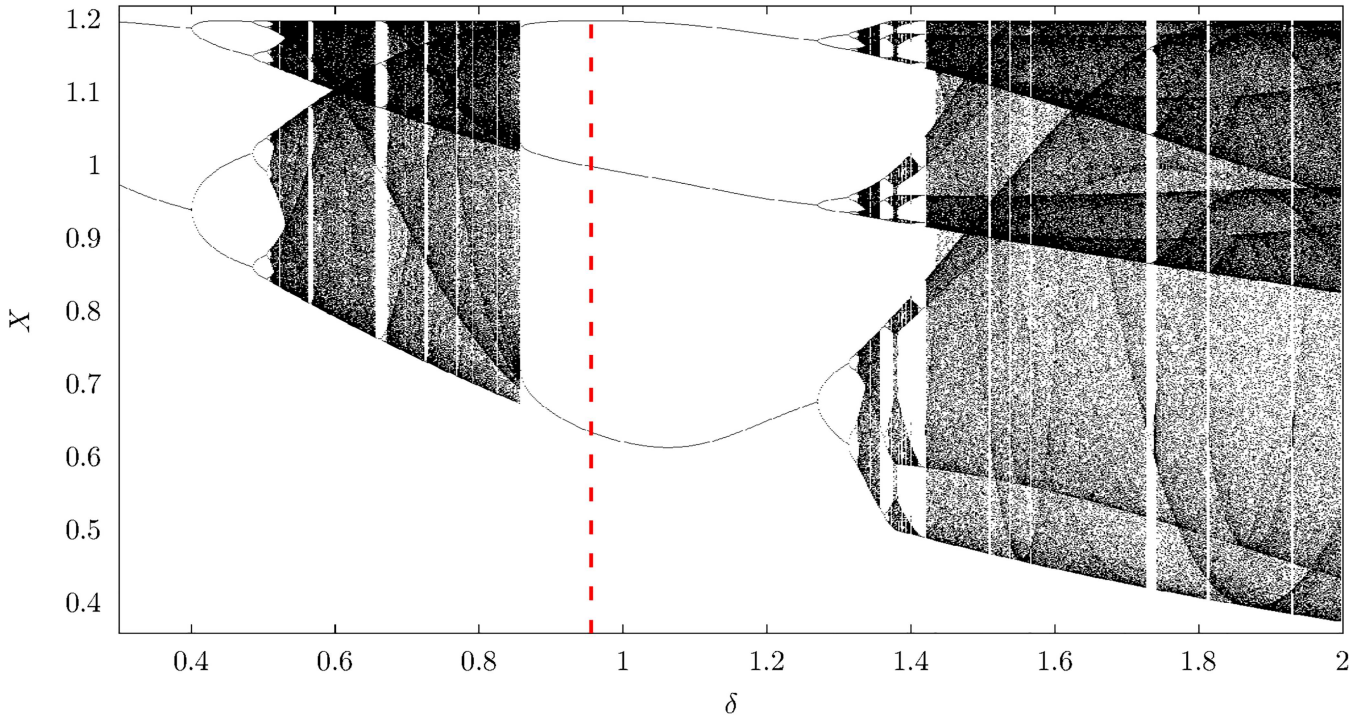


FIG. 5. Bifurcation diagram X vs δ following the dashed line that was shown in Fig. 4(d). Here, we can see that there are some duplications of period that lead us to chaotic attractors. These chaotic regions have windows of periodicity that correspond to CSP structures. The red dashed line has the same parameters as the red circle highlighted in Fig. 4(d).

red to yellow represents negative Lyapunov exponents (indicative of periodic orbits), while the color transitions from green to blue signify positive Lyapunov exponents (associated with chaotic orbits). In this figure, the periodic regions are embedded within chaotic regions, and superstable curves ($\lambda \ll 0$) appear in red within the yellow areas. We will focus our study on the region delimited by the rectangle in the bottom-left corner of Fig. 1 due to the presence of periodic structures in this area. In Secs. III A–III E, we will analyze this region in more detail for different values of the β parameter.

A. Results for $\beta = 0.1$

In this section, we will present some results for $\beta = 0.1$; for this, we construct the parameter space presented in Fig. 2(a), which corresponds to the region delimited in Fig. 1. We highlight superstable curve $[3]^r$ illustrated in red. In this case, $u = 3$ (period 3) and $i = r$, indicating that $X_{(r)}$, after three iterations, returns to itself. Additional superstable curves are highlighted in Fig. 2(a), labeled as $[2]^r$, $[2]^m$, $[3]^m$, $[4]^r$, and $[4]^m$. It is noteworthy that all these curves are within a periodic region with high negative values of λ.

In Fig. 2(b), we adjusted the color palette: periodic structures are highlighted in gray ($\lambda < 0$), while white represents chaotic regions ($\lambda > 0$). Figure 2(b) displays several extreme curves note that, unlike the superstable curve notation using square brackets, extreme curves are denoted with parentheses. For instance, in Fig. 2(b), we have the extreme curve $(2)^{rm}$, where $u = 2$, $i = r$, and $j = m$. Therefore, an extreme orbit related to this extreme curve starts at $F(X_{(r)}) \equiv Y_r$ and, after two iterations, reaches $F(X_{(m)}) \equiv Y_m$. To illustrate the distinction between superstable and extreme curves, we use the return maps shown in Fig. 3 and constructed for the parameters related to the red, blue, and green points highlighted in Fig. 2.

Figure 3(a) illustrates an example of an extreme orbit that connects the local maximum $Y_{(r)}$ to the minimum $Y_{(m)}$ after iterating the mapping twice; hence, the extreme curve associated with that orbit is denoted as $(2)^{rm}$. In Fig. 3(b), we observe the outcome of iterating the mapping after reaching the local minimum $Y_{(m)}$. Notably, the blue orbit, after a single iteration, returns to the local maximum $Y_{(r)}$, exemplifying an extreme orbit associated with the extreme curve $(1)^{mr}$. Additionally, it is evident that this orbit departs from a maximum at $Y_{(r)}$ and, after three iterations, returns to the same position, constituting a superstable orbit of period 3 associated with the superstable $[3]^r$. A similar phenomenon occurs when considering $Y_{(m)}$ as the initial condition. Iterating the mapping three times results in the trajectory returning to the minimum at $X_{(m)}$, in this case the orbit is associated with superstable $[3]^m$. Therefore, Fig. 3(b) reveals the coexistence of two extreme orbits composing a superstable orbit with two critical points of the map. We can summarize the observations in Figs. 3(a) and 3(b) with the following properties:

19 February 2025 18:39:51

Published under an exclusive license by AIP Publishing

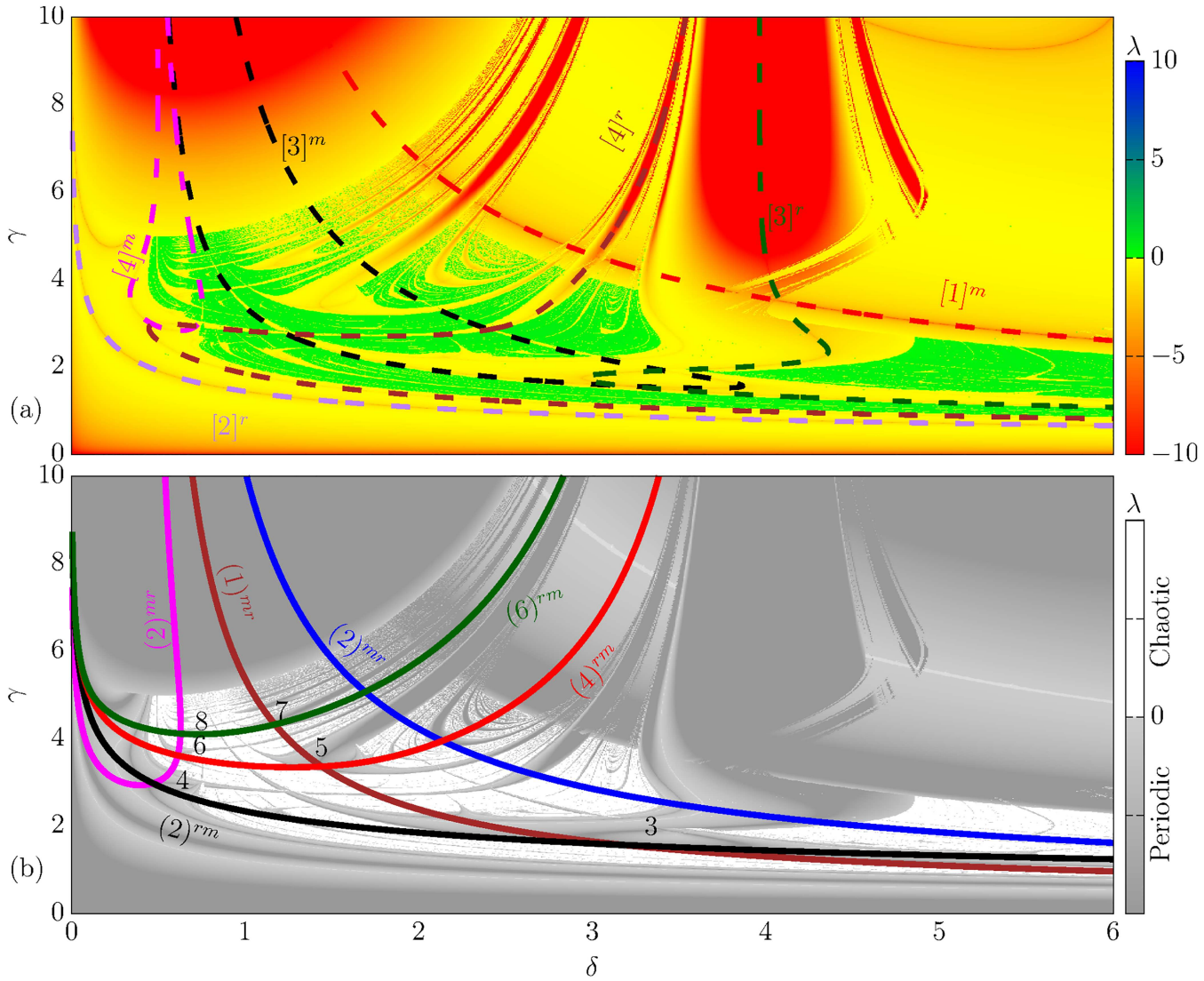


FIG. 6. Parameter space γ vs δ for $\beta = 0.3$, where the color scheme represents the value of the Lyapunov exponent λ. The dashed lines in (a) are named as superstable curves, while the lines in (b) are named as extreme curves. The numbers in (b) correspond to the periodicity of the CSP structures.

Property 1. Let $(u)^{ij}$ and $(v)^{ji}$ be two extreme curves ($i \neq j$). If they coexist for a singular combination of control parameters, then they also coexist with two other superstable curves $[u+v]^i$ and $[u+v]^j$ and a superstable periodic orbit, period $u+v$, takes place with both critical points X_i and X_j.

Note that for $i \neq j$, a superstable orbit exists when the u and v-extreme orbits, where $X_i = F^{(u)}(X_j)$ and $X_j = F^{(v)}(X_i)$, respectively, occur simultaneously, since $X_i = F^{(u)}(X_j) = F^{(u)}(F^{(v)}(X_i)) = F^{(u+v)}(X_i)$. That is, $X_i = F^{(u+v)}(X_i)$, a superstable orbit period $u+v$. This shows that in the state space, the u and v-extreme orbits compose a double $[F^{u+v}(X_i)$ and $F^{u+v}(X_j)]$ superstable periodic orbit. On the other hand, in the parameter space, the coexistence of extreme and superstable curves occurs for a singular combination of control parameters.

To illustrate Property 1, in Fig. 3(a), we have an extreme orbit associated to curve $(2)^{rm}$ highlighted in red, connecting X_r to X_m after two iterations. Meanwhile, in Fig. 3(b), in addition to the orbit already highlighted, we have in blue an extreme orbit associated to curve $(1)^{mr}$, i.e., connecting X_m to X_r after one iteration. It is worth noting that the beginning of one orbit coincides with the end of the other, generating a superstable orbit of period 3, where X_m (or X_r) returns to itself after three iterations, as predicted by Property 1.

19 February 2025 18:39:51

Published under an exclusive license by AIP Publishing

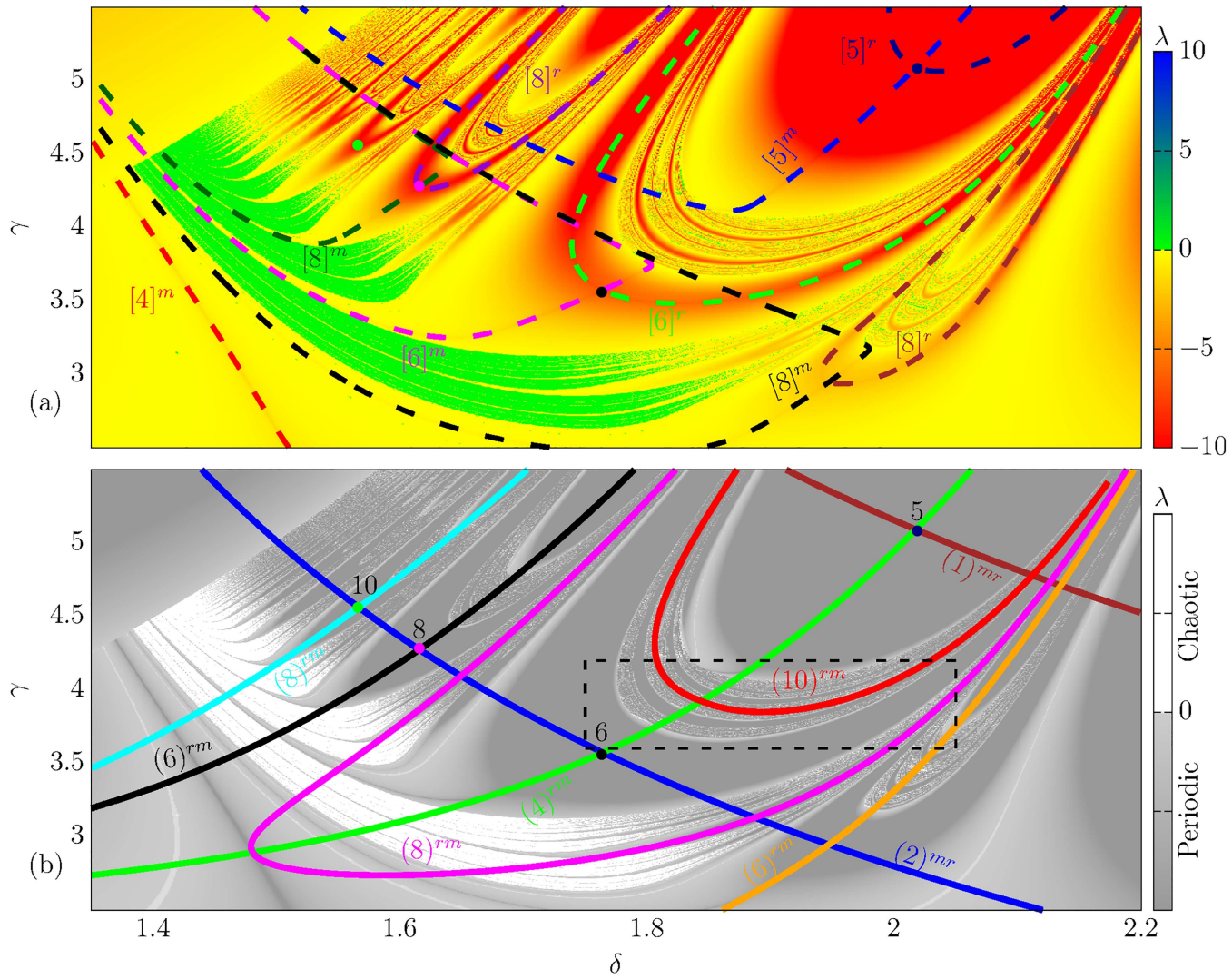


FIG. 7. Parameter space γ vs δ for $\beta = 0.5$, where the color scheme represents the value of the Lyapunov exponent λ. The dashed lines in (a) are named as superstable curves, while the lines in (b) are named as extreme curves.

Additionally, in the parameter space shown in Fig. 2(b), we highlight in blue the point where the extreme curves $(2)^{rm}$ and $(1)^{mr}$ coexist. This same point is highlighted in Fig. 2(a), where some superstable curves are traced. It is observed that at this point, two superstable curves also coexist, $[3]^r$ and $[3]^m$, as described by Property 1.

To generate Figs. 3(c) and 3(d), the following parameters were considered: $\delta = 0.1353$, $\gamma = 9.7165$, and $\beta = 0.1$ [these parameters correspond to the red dot in the parameter space shown in Figs. 2(a) and 2(b)]. In Fig. 3(c), the curve $(2)^{rm}$ is depicted in red, while in Fig. 3(d), we illustrate the outcome after iterating the map several times. In this case, the blue lines represent a chaotic attractor. Therefore, this combination of control parameters leads to the coexistence of an extreme orbit with a chaotic attractor. Note that Property 1 is not applicable in this scenario since we have only one extreme curve.

In Figs. 3(e) and 3(f), we utilized the following parameters: $\delta = 0.352\,08$, $\gamma = 4.235\,32$, and $\beta = 0.1$ (where these parameters correspond to the green dot in Fig. 2). Figure 3(e) displays the curve $(1)^{mr}$ in red, connecting the minimum $Y_{(m)}$ to the maximum $Y_{(r)}$ after one iteration. In Fig. 3(f), the curve $(3)^{mr}$ in blue is shown, which, after three iterations, departs from the minimum $Y_{(m)}$, and reaches the maximum $Y_{(r)}$. Observe the existence of a closed rectangle that connects the local maximum at $Y_{(r)}$ to itself after two iterations. This exemplifies a superstable orbit named as $[2]^r$. With this example in mind, we propose the following property:

19 February 2025 18:39:51

Published under an exclusive license by AIP Publishing

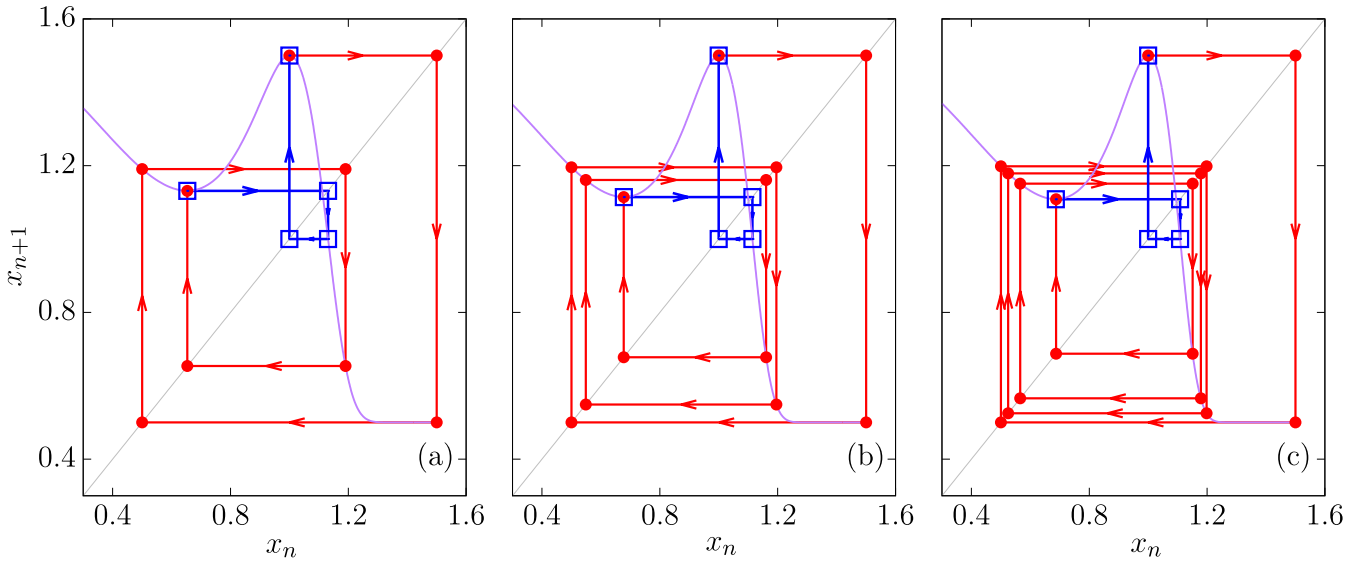


FIG. 8. In (a), we show an orbit associated with the extreme curve $(4)^{rm}$ in red, and an other orbit associated with the curve $(2)^{mr}$ in blue, where this figure corresponds to the black point/circle in Figs. 7(a) and 7(b). The union of these two orbits creates a superstable orbit with period 6. In item (b), we highlight an orbit associated with the extreme curve $(6)^{rm}$ (in red) and an other orbit associated with the extreme curve $(2)^{mr}$ (in blue), where this figure corresponds to the magenta point/circle of Figs. 7(a) and 7(b). Item (c), we have an orbit associated with the extreme curve $(8)^{rm}$ (in red) and an orbit associated with the extreme curve $(2)^{mr}$ (in blue). This figure corresponds to the green dot in Figs. 7(c) and 7(b). We used the following combination of control parameters: (a) $\delta = 1.7645$ and $\gamma = 3.5722$; (b) $\delta = 1.6156$ and $\gamma = 4.2739$; and (c) $\delta = 1.5668$ and $\gamma = 4.5606$. For all situations, we have $\beta = 0.5$.

Property 2. Let $(u)^{ij}$ and $(v)^{ij}$ [in contrast with $(v)^{ji}$ considered in Property 1] be two extreme curves with $(i \neq j)$, where $u > v$, and no $(w)^{ij}$ with $v < w < u$ exists. If they coexist for a singular combination of control parameters, they also coexist with one of the superstable curves $[u-v]^j$ or $[u-v]^i$.

To explain this, consider the u and v-extreme orbits, where, respectively, $X_i = F^{(u)}(X_j)$ and $X_i = F^{(v)}(X_j)$, with $u > v$. Then, $X_i = F^{(v)}(X_j) = F^{(u)}(X_j) = F^{(u-v+v)}(X_j) = F^{(u-v)}(F^{(v)}(X_j)) = F^{(u-v)}(X_i)$, indicating that $X_i = F^{(u-v)}(X_i)$. Since there is no w in between v and u, this result corresponds to a superstable orbit period $u-v$. This situation is illustrated in Figs. 3(e) and 3(f), where we observe two extreme orbits that combine to form a periodic orbit of period 2. The first orbit connects the minimum $Y_{(m)}$ to the maximum $Y_{(r)}$ after three iterations, while the second connects $Y_{(m)}$ to $Y_{(r)}$ after one iteration. Additionally, this behavior is reflected in the parameter space. In Fig. 2(a), the extreme curves $(3)^{mr}$ and $(1)^{mr}$ intersect in a region that does not correspond to the center of a periodic structure. Instead, they intersect a superstable curve with periodicity 2, as indicated by the green intersection point in Figs. 2(a) and 2(b).

B. Results for $\beta = 0.2$

Continuing with the analysis, we now consider the value of $\beta = 0.2$. To do this, we constructed the parameter spaces shown in Fig. 4. For this β value, we noticed the emergence of two regions of great stability painted in red. In Fig. 4(a), we observe some superstable curves such as the curve $[3]^r$, embedded within a red region (periodic region). This curve, on both sides (left and right), is followed by two superstable curves $[4]^r$. On the left of them, we notice two superstable curves, $[1]^m$ and $[2]^m$, heading toward the same red region (periodic region). Figure 4(b) presents a similar plot to Fig. 4(a), utilizing a different color palette to distinguish chaotic and periodic regions, using the same color palette as Fig. 2(b). In Fig. 4(b), we highlight some extreme curves, named as $(1)^{mr}$, $(2)^{mr}$, $(2)^{rm}$, $(4)^{rm}$, and $(6)^{rm}$.

For a more detailed analysis, we enlarge the region marked by a rectangle in the bottom-left corner of Fig. 4(b). This magnification is shown in Figs. 4(c) and 4(d) and allows us to observe with greater precision aspects that were not previously evident, such as cascades of CSP structures. In Fig. 4(d), we observe the following extreme curves: $(1)^{mr}$, $(2)^{mr}$, $(2)^{rm}$, $(4)^{rm}$, and $(6)^{rm}$. Additionally, in this figure, one can notice the alignment of CSP structures from the extreme curve $(1)^{mr}$, followed by CSP structures with periods $3, 5, 7$, and so on, accumulating in a domain of periodicity 2 (top-left corner of the figure). It is noteworthy that, in Fig. 4(d), the extreme curves $(1)^{mr}$ and $(2)^{rm}$ intersect each other in a period 3 CSP structure (red-colored point). This intersection, in accordance with Property 1, occurs at the exact location where two superstable curves also coexist, named as $[3]^r$ and $[3]^m$ in Fig. 4(c).

19 February 2025 18:39:51

Published under an exclusive license by AIP Publishing

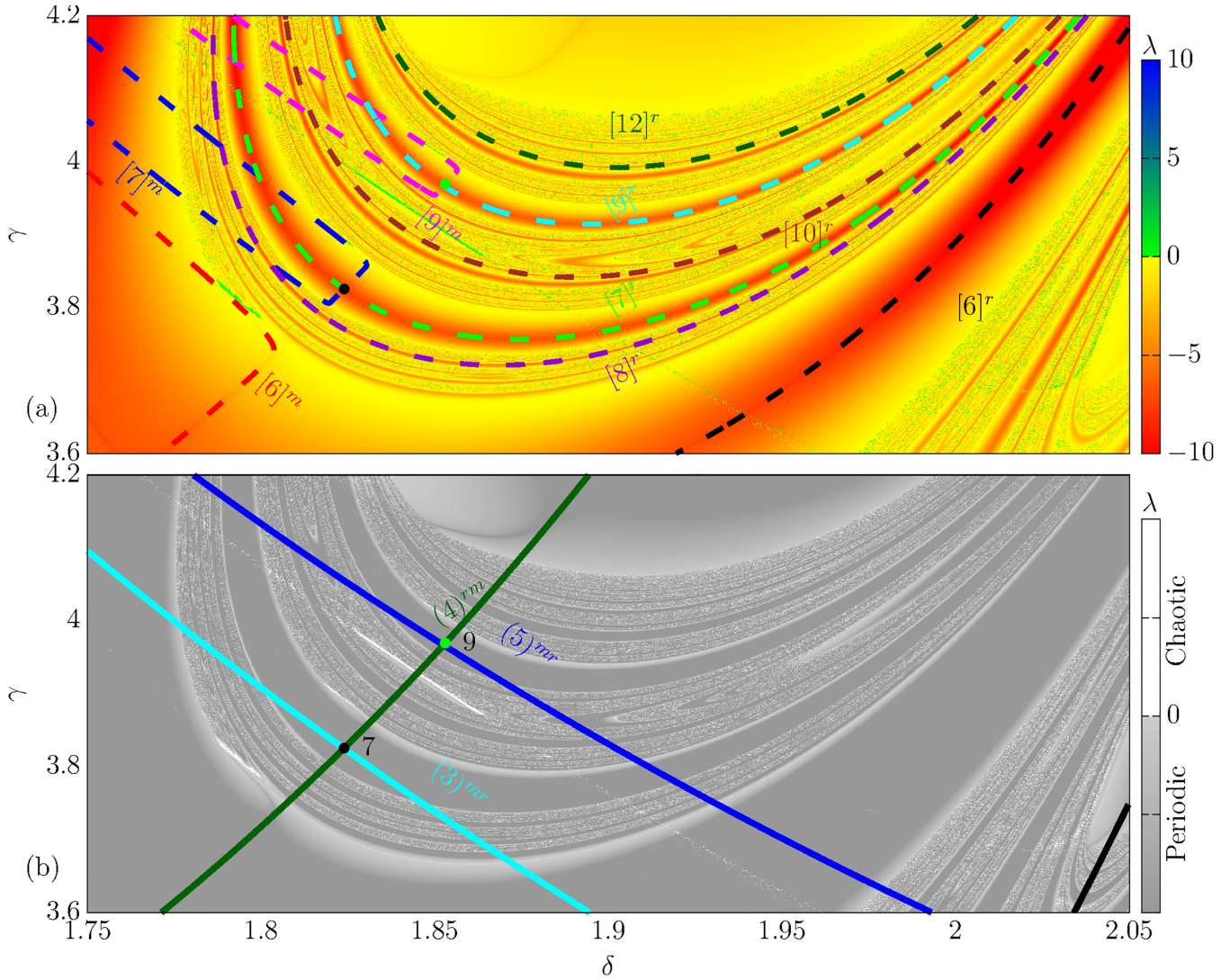


FIG. 9. Parameter space γ vs δ for fixed value of $\beta = 0.5$, where the color scheme represents the value of the Lyapunov exponent. The dashed lines in (a) are named as superstable curves while the lines in (b) are the extreme curves.

In order to deepen our analysis of the dynamics in the vicinity of a CSP structure, we draw the bifurcation diagram X vs δ shown in Fig. 5. In this diagram, we draw a red dashed line corresponding to the point marked in red in Fig. 4(d), which is the intersection of the extreme curves $(2)^{rm}$ and $(1)^{mr}$. Note that the red line intersects a period 3 structure in the bifurcation diagram, corresponding to the period of the CSP structure that contains the point of intersection of the extreme curves. Again in accordance with Property 1. Furthermore, both to the right and left of the red line, we have periodicity windows along chaotic regions that correspond to other CSP structures shown in the parameter space of Fig. 4(d) immersed in chaos.

C. Results for $\beta = 0.3$

Transitioning to $\beta = 0.3$ yields the results depicted in Figs. 6(a) and 6(b). Figure 6(b) illustrates the coherent alignment of CSPs along the trajectory of the extreme curve $(1)^{mr}$. Notably, this alignment is accompanied by another set of CSPs with periodicities of 4, 6, 8, and so forth, systematically organized by the extreme curve $(2)^{mr}$. These structures follow a sequence of period duplications, ultimately leading to chaos through Feigenbaum's Universality.[20] In Fig. 6(b), the intersection of extreme curves $(1)^{mr}$ with $(2)^{rm}$ and $(2)^{rm}$ with $(2)^{mr}$ is apparent. Both intersections manifest as CSP structures with periodicities of 3 and 4, respectively, which shows the validity of Property 1 also for $\beta = 0.3$.

19 February 2025 18:39:51

Published under an exclusive license by AIP Publishing

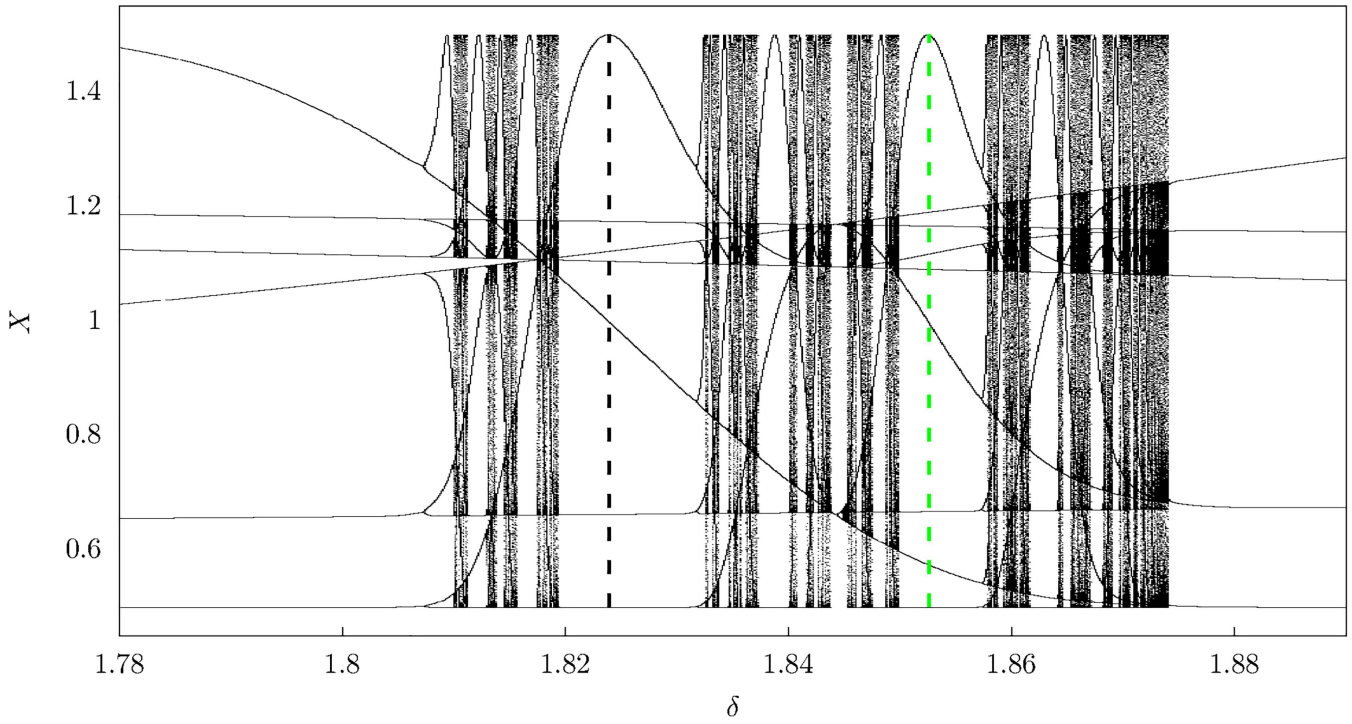


FIG. 10. Bifurcation diagram X vs δ following the $(4)^{rm}$ curve of Fig. 9(b). Here, we can see some periodic regions along with chaotic regions. These chaotic regions have periodicity windows, which are periodic regions that correspond to CSP structures. The black and green dotted lines have the same parameters as the black and green point/circle highlighted in Figs. 9(a) and 9(b).

D. Results for $\beta = 0.5$

Exploring $\beta = 0.5$, we observe in Fig. 7(b), a period-adding sequence of CSPs aligned with the trajectory of the extreme curve $(2)^{mr}$. These CSPs exhibit periodicities of 6, 8, 10, and so forth, consistently incrementing by two units compared to the preceding periodicity. Additionally, we emphasize the intersection of extreme curves $(1)^{mr}$ and $(4)^{rm}$ at a period 5 CSP. Notably, in accordance with Property 1, these curves intersect two superstable curves denoted as $[5]^r$ and $[5]^m$. Intriguing superstable curves, including $[5]^r$, $[6]^r$, and $[8]^r$, are depicted in Fig. 7(a). These curves are prominently situated within vibrant red-colored regions, indicative of periodic regions. Additionally, overlapping occurs for the curves $[6]^m$ and $[8]^m$ beyond a specific point.

In Fig. 8, we present plots of X_1 vs X_0 corresponding to the intersections highlighted in Fig. 7. For Fig. 8(a), we selected the following parameters: $\delta = 1.7645$, $\gamma = 3.5722$, and $\beta = 0.5$, represented by the black circle in Figs. 7(a) and 7(b). The red curve in this figure illustrates an orbit associated with the extreme curve $(4)^{rm}$ connecting a local maximum X_r to a local minimum X_m after four iterations. Simultaneously, the blue curve represents an orbit associated with the extreme curve $(2)^{mr}$ departing from a local minimum X_m and reaching a maximum at X_r after two iterations. Remarkably, the termination of an orbit coincides with the initiation of other, resulting in a closed orbit with a period of 6. This intersection point witnesses the coexistence of the superstable curves $[6]^m$ and $[6]^r$, as observed in Fig. 7(a). It is crucial to highlight that this outcome aligns with Property 1.

Turning our attention to Fig. 8(b), we consider the parameter set $\delta = 1.6156$, $\gamma = 4.2739$, and $\beta = 0.5$, corresponding to the magenta circle in Figs. 7(a) and 7(b). Here, the red curve illustrates an orbit associated with the extreme curve $(6)^{rm}$, originating from a local maximum X_r and concluding at a local minimum X_m after six iterations. Simultaneously, the blue curve represents an orbit associated with the extreme curve $(2)^{mr}$, exhibiting the same behavior as described in the context of Fig. 8(a). The combination of these two extreme orbits results in a closed orbit with a period of 8. Notably, the intersection point of the two extreme curves aligns precisely with the intersection between the superstable curves $[8]^r$ and $[8]^m$. This observation solidifies the coexistence of the corresponding superstable curves at this specific spatial arrangement.

Considering Fig. 8(c), the parameter set $\delta = 1.5668$, $\gamma = 4.5606$, and $\beta = 0.5$ is explored, corresponding to the green circles in Figs. 7(a) and 7(b). In this illustration, the red curve represents an orbit associated with the extreme curve $(8)^{rm}$, portraying the orbit's trajectory from a local maximum at $X_{(r)}$ to a local minimum at $X_{(m)}$ after eight iterations. The blue curve, an orbit associated with

19 February 2025 18:39:51

Published under an exclusive license by AIP Publishing

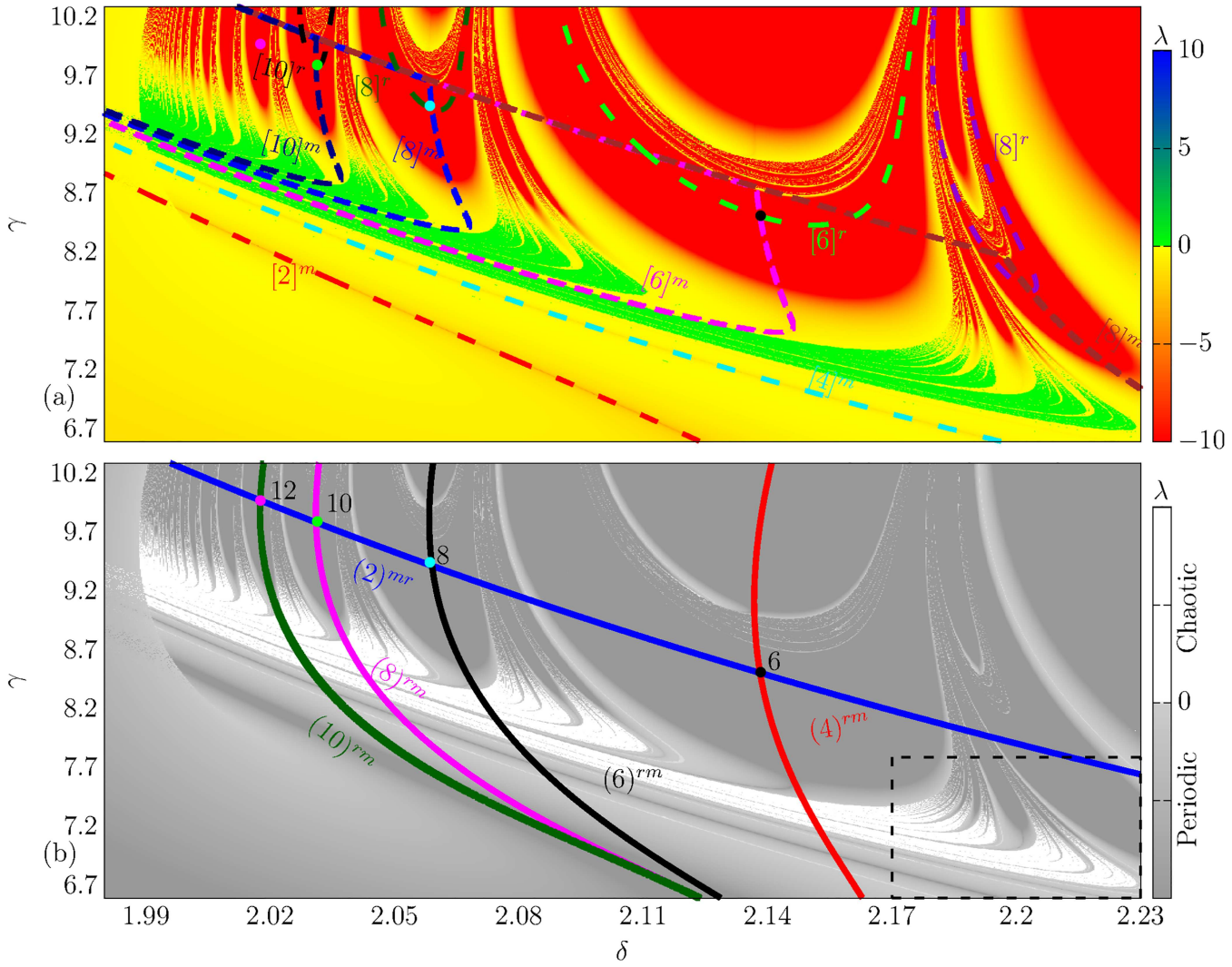


FIG. 11. Parameter space γ vs δ for $\beta = 0.7$, where the color scheme represents the value of the Lyapunov exponent λ. The dashed lines in (a) are named as superstable curves, while the lines in (b) are named as extreme curves.

the curve $(2)^{mr}$, adheres to a behavior analogous to that discussed in Figs. 8(a) and 8(b). The union of these two extreme orbits, forming a closed orbit, aligns with the expectation outlined in Property 1, emphasizing the coexistence of superstable curves. Consequently, the intersection of the extreme curves $(8)^{rm}$ and $(2)^{mr}$ corresponds to a period-10 Complex Set of Periodicity (CSP).

Still for beta = 0.5, we analyzed Fig. 9 which corresponds to a magnification of the area enclosed by the dotted rectangle in Fig. 7, providing a detailed view of the events occurring in that specific region. In Fig. 9(b), the green curve represents the extreme curve $(4)^{rm}$ intersecting with two other extreme curves, specifically, $(3)^{mr}$ and $(5)^{mr}$. A closer inspection in Fig. 9(a) reveals the intersections of the superstable curves $[7]^r$ with $[7]^m$ and also the intersections of the curves $[9]^r$ with $[9]^m$, consistently adhering to the established definitions.

Examining Fig. 10, the bifurcation diagram X vs β unfolds as we track the trajectory of the extreme curve $(4)^{rm}$ [highlighted in Fig. 9(b)]. The diagram presents a sequence of events progressing from left to right. Initiating with a period of 6, validated by the presence of the superstable curve $[6]^m$ traversing the lower-left corner in Fig. 9(a), the system delves into chaotic regions interspersed with periodicity windows. A distinctive region featuring a period of 7 is marked by a black dashed line, corresponding to the black circle in Figs. 9(a) and 9(b). Subsequently, the system reenters chaotic attractors, accompanied by periodicity windows, until reaching another region exhibiting a period of 9. This specific segment is delineated

19 February 2025 18:39:51

Published under an exclusive license by AIP Publishing

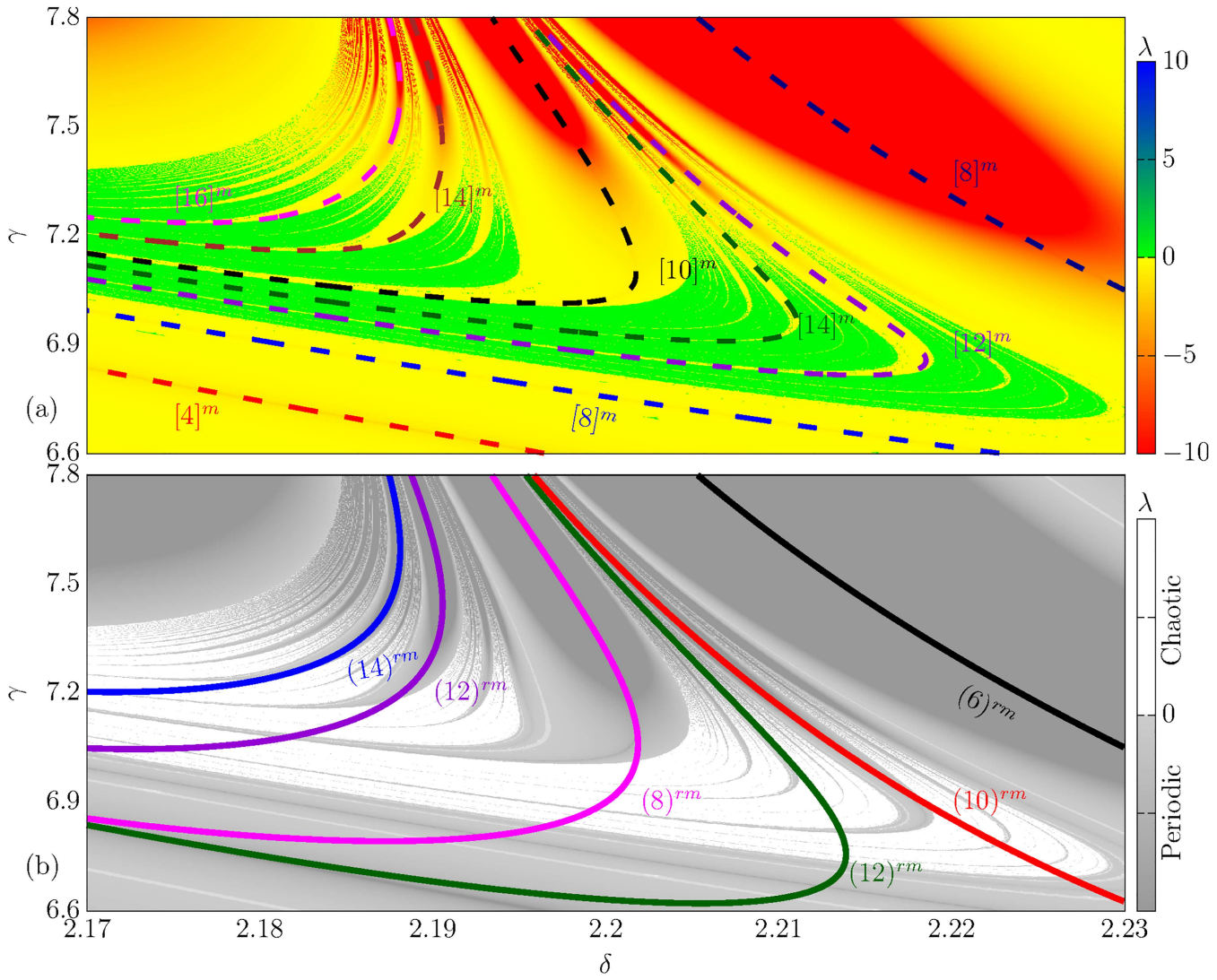


FIG. 12. Parameter space γ vs δ for fixed value of $\beta = 0.7$, where the color scheme represents the value of the Lyapunov exponent. The dashed lines in (a) are named as superstable curves, while the lines in (b) are the extreming curves.

by a green dashed line, corresponding to the green circle in Figs. 9(a) and 9(b).

E. Results for $\beta = 0.7$

Considering $\beta = 0.7$, the outcomes revealed in Fig. 11 shed light on the intricate dynamics of the system. Particularly, in Fig. 11(b), attention is drawn to the pronounced features of the extreme curve $(2)^{mr}$ as it intersects with other extreme curves, including $(4)^{rm}$, $(6)^{rm}$, $(8)^{rm}$, $(10)^{rm}$, and subsequent structures. This sequence of intersections follows a period-adding pattern, with each subsequent structure incorporating an additional two units to its periodicity (e.g., 8, 10, and 12). The detailed organization of Complex Sets of Periodicity (CSPs) in Fig. 11(a) reinforces the periodic nature of these structures, with intersecting superstable curves like $[6]^r$ with $[6]^m$, $[8]^r$ with $[8]^m$, and $[10]^r$ with $[10]^m$. The overlapping of superstable curves $[6]^m$, $[8]^m$, and $[10]^m$ with $[8]^m$ is notably discernible, particularly within the red-colored regions exhibiting Lyapunov exponents below -10.

In the bifurcation diagram portrayed in Fig. 13, tracking the trajectory along the curve $(2)^{mr}$ provides crucial insights that corroborate the findings in Fig. 11. Examining the diagram from right to left, a distinct pattern emerges: an initial period of 8 gives way to chaotic regions interspersed with periodic windows. Subsequently, a

19 February 2025 18:39:51

Published under an exclusive license by AIP Publishing

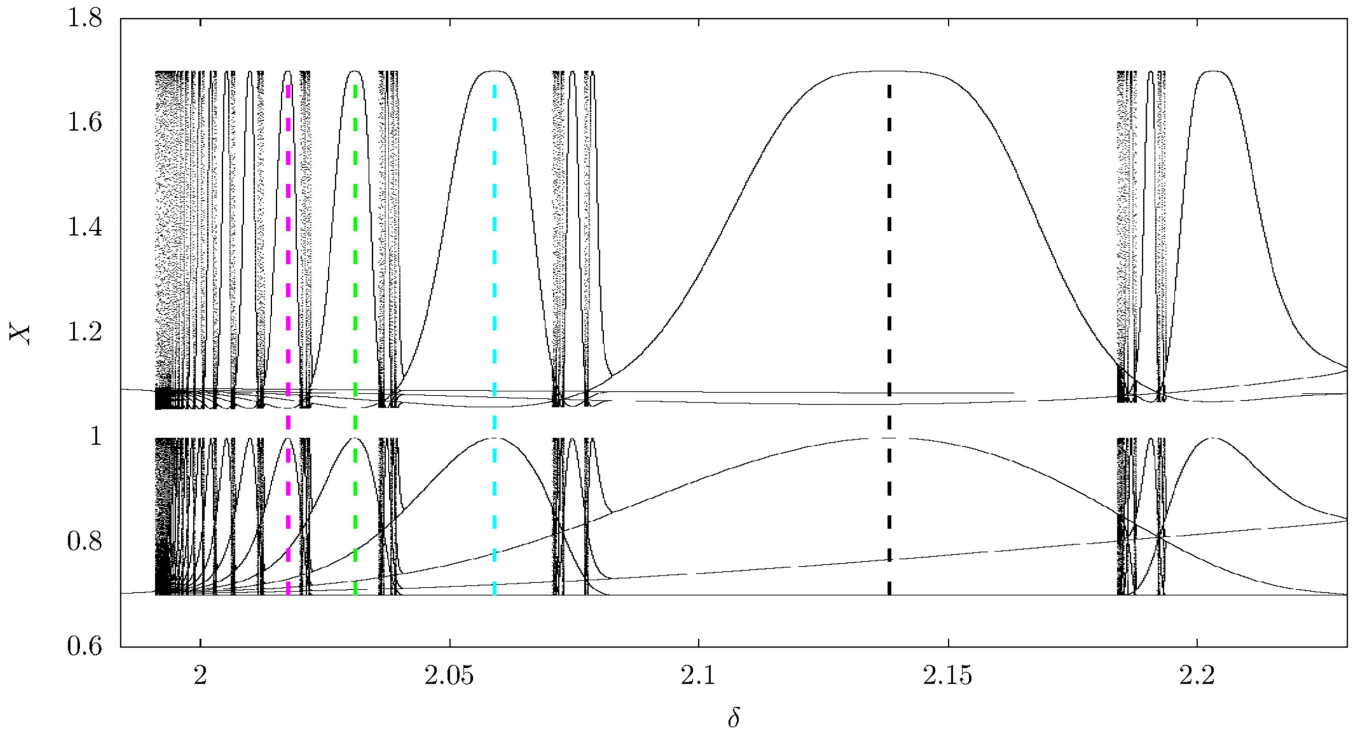


FIG. 13. Bifurcation diagram X vs δ following the $(2)^{mr}$ curve of Fig. 11(b). Here, we can see some periodic regions along with chaotic regions. These chaotic regions have periodicity windows, which are periodic regions that correspond to CSP structures. The black, red, green, and magenta dotted lines have the same parameters as the black, cyan, green, and magenta point/circle highlighted in Figs. 11(a) and 11(b).

region with periodicity 6 is identified, depicted by the black dashed line aligning with the black circles in Figs. 11(a) and 11(b). The sequence continues with further oscillations between chaotic and periodic regimes, culminating in a region of periodicity 8 (cyan dashed line), aligning with the cyan circles in Figs. 11(a) and 11(b). This pattern persists until a region of periodicity 2 is reached, affirming the presence of a period-adding sequence orchestrated by the extreme curve $(2)^{mr}$.

Turning attention to Fig. 12, which magnifies the lower right corner of Fig. 11(b), specific extreme curves such as $(6)^{rm}$, $(8)^{rm}$, $(10)^{rm}$, and $(12)^{rm}$ are highlighted. Remarkably, these curves exclusively traverse between local maxima (X_r) and minima (X_m) due to the absence of complete Complex Sets of Periodicity (CSP) structures within this region. This observation is supported by Fig. 12(a), where superstable curves predominantly navigate from the local minimum X_m back to itself after a specific number of iterations. Hence, the analogous behavior across structures in Fig. 11 akin to the highlighted region in Fig. 12 becomes evident.

IV. CONCLUSIONS

In this study, we explored the one-dimensional composed Logistic–Gauss map. As previously documented, this mapping exhibits intriguing dynamic properties. Our main objective was to comprehend the transformations occurring when adjusting the system's control parameters. By varying these parameters, we observed changes in the characteristics of Complex Sets of Periodicity (CSPs).

Utilizing the theory of extreme curves, we introduced two significant properties that elucidate dynamics in the parameter space. These properties provide detailed insights into intersections between extreme and superstable curves, outlining conditions for the coexistence of these structures.

Bifurcation diagrams were crucial tools for characterizing orbits associated with the considered intersections of superstable and extreme curves. Additionally, we highlighted the presence of sequences of period duplications when following specific extreme orbits, revealing connections with Feigenbaum's Universality and showcasing the transition to chaotic behavior.

This comprehensive approach has improved our understanding of the complex dynamics in the Composed Logistic–Gauss map, offering a clearer view of system behavior in response to variations in control parameters. Reinforcing the idea that this approach can be used in other models.

ACKNOWLEDGMENTS

L.S.d.P. and J.G.S.R. acknowledge Coordenação de Aperfeiçoamento de Pessoal de Nível Superior—Brasil (CAPES). D.R.d.C., R.L.V., and I.L.C. acknowledge the São Paulo Research Foundation (FAPESP, Brazil) (Grants Nos. 2020/02415-7, 2019/09150-1, and 2018/03211-6) and National Council for Scientific and Technological

19 February 2025 18:39:51

Published under an exclusive license by AIP Publishing

Development (CNPq) (Grants Nos. 162944/2020-0 and 301019/2019-3). J.D.V.H. thanks Federal Institute of Education, Science and Technology of South of Minas Gerais—IFSULDEMINAS. R.O.M.-T. acknowledges the São Paulo Research Foundation (FAPESP, Proc. No. 2015/50122-0 and Grant No. 2024/06718-5) and National Council for Scientific and Technological Development (CNPq), Proc. No. 408522/2023-2. M.H. is funded by national funds through the FCT—Fundação para a Ciência e a Tecnologia, I.P., under the scope of Project Nos. UIDB/00297/2020 (https://doi.org/10.54499/UIDB/00297/2020) and UIDP/00297/2020 (https://doi.org/10.54499/UIDP/00297/2020) (Center for Mathematics and Applications).

AUTHOR DECLARATIONS

Conflict of Interest

The authors have no conflicts to disclose.

Author Contributions

Luam Silva de Paiva: Conceptualization (equal); Data curation (equal); Formal analysis (equal); Funding acquisition (equal); Investigation (equal); Methodology (equal); Software (equal); Validation (equal); Visualization (equal); Writing – original draft (equal); Writing – review & editing (equal). **Julia G. S. Rocha:** Conceptualization (equal); Data curation (equal); Formal analysis (equal); Investigation (equal); Writing – original draft (equal); Writing – review & editing (equal). **Joelson D. V. Hermes:** Conceptualization (equal); Formal analysis (equal); Investigation (equal); Software (equal); Validation (equal); Writing – original draft (equal); Writing – review & editing (equal). **Matheus Hansen:** Conceptualization (equal); Formal analysis (equal); Methodology (equal); Writing – original draft (equal); Writing – review & editing (equal). **Ricardo Luiz Viana:** Conceptualization (equal); Methodology (equal); Supervision (equal); Writing – original draft (equal); Writing – review & editing (equal). **Iberê Luiz Caldas:** Conceptualization (equal); Methodology (equal); Supervision (equal); Writing – original draft (equal); Writing – review & editing (equal). **Rene O. Medrano-T:** Conceptualization (equal); Methodology (equal); Supervision (equal); Writing – original draft (equal); Writing – review & editing (equal). **Diogo Ricardo da Costa:** Conceptualization (equal); Formal analysis (equal); Investigation (equal); Software (equal); Supervision (equal); Writing – original draft (equal); Writing – review & editing (equal).

DATA AVAILABILITY

The data that support the findings of this study are available from the corresponding author upon reasonable request.

REFERENCES

[1]M. Kesmia, S. Boughaba, and S. Jacquir, "Nonlinear dynamics of two-dimensional cardiac action potential duration mapping model with memory," J. Math. Biol. **78**, 1529–1552 (2019).
[2]S. Tanabe and N. Masuda, "Complex dynamics of a nonlinear voter model with contrarian agents," Chaos **23**, 043136 (2013).
[3]A. S. Reis, K. C. Iarosz, F. A. Ferrari, I. L. Caldas, A. M. Batista, and R. L. Viana, "Bursting synchronization in neuronal assemblies of scale-free networks," Chaos Solitons Fractals **142**, 110395 (2021).
[4]R. May, "Simple mathematical models with very complicated dynamics," Nature **261**, 459–467 (1976).
[5]D. R. da Costa, M. Hansen, E. D. Leonel, and R. O. Medrano-T, "Extreming curves and the parameter space of a generalized logistic mapping," J. Vib. Testing Syst. Dyn. **2**(2), 109–118 (2018).
[6]Z. Zhou, W. Shi, Y. Bao, and M. Yang, "A Gaussian function based chaotic neural network," in *2010 International Conference on Computer Application and System Modeling (ICCASM 2010)* (IEEE, 2010), Vol. 4, pp. V4–203.
[7]J. A. de Oliveira, H. M. de Mendonça, A. A. da Silva, and E. D. Leonel, "Critical slowing down at a fold and a period doubling bifurcations for a Gauss map," Braz. J. Phys. **49**, 923–927 (2019).
[8]D. R. da Costa, J. G. Rocha, L. S. de Paiva, and R. O. Medrano-T, "Logistic-like and Gauss coupled maps: The born of period-adding cascades," Chaos Solitons Fractals **144**, 110688 (2021).
[9]D. R. Da Costa, M. Hansen, G. Guarise, R. O. Medrano-T, and E. D. Leonel, "The role of extreme orbits in the global organization of periodic regions in parameter space for one dimensional maps," Phys. Lett. A **380**, 1610–1614 (2016).
[10]C. E. P. Abreu, J. D. V. Hermes, D. R. da Costa, E. S. Medeiros, and R. O. Medrano-T, "Extreme fractal dimension at periodicity cascades in parameter spaces," Phys. Rev. E **110**, L032201 (2024).
[11]S. Fraser and R. Kapral, "Analysis of flow hysteresis by a one-dimensional map," Phys. Rev. A **25**, 3223 (1982).
[12]R. Vitolo, P. Glendinning, and J. A. C. Gallas, "Global structure of periodicity hubs in Lyapunov phase diagrams of dissipative flows," Phys. Rev. E **84**, 016216 (2011).
[13]E. Lorenz, "Compound windows of the Hénon map," Physica D **237**, 1689 (2008).
[14]C. Mira, *Chaotic Dynamics* (World Scientific, Singapore, 1987).
[15]S. V. Gonchenko, C. Simó, and A. Vieiro, "Richness of dynamics and global bifurcations in systems with a homoclinic figure-eight," Nonlinearity **26**, 621 (2013).
[16]J. A. De Oliveira, L. T. Montero, D. R. Da Costa, J. Méndez-Bermúdez, R. O. Medrano-T, and E. D. Leonel, "An investigation of the parameter space for a family of dissipative mappings," Chaos **29**, 053114 (2019).
[17]D. M. Maranhão and R. O. Medrano-T, "Periodicity in the asymmetrical quartic map," Chaos Solitons Fractals **186**, 115204 (2024).
[18]C. A. T. Chávez and S. Curilef, "Tricorn-like structures in an optically injected semiconductor laser," Chaos **30**, 023130 (2020).
[19]R. O. Medrano-T and R. Rocha, "The negative side of Chua's circuit parameter space: Stability analysis, period-adding, basin of attraction metamorphoses, and experimental investigation," Int. J. Bifurcat. Chaos **24**, 1430025 (2014).
[20]M. J. Feigenbaum, "Universal behavior in nonlinear systems," Phys. D **7**, 16–39 (1983).

19 February 2025 18:39:51

Published under an exclusive license by AIP Publishing